

Relaxation behavior of hydrophobically modified polyelectrolyte solution under various deformations

K.C. Tam^{a,*}, W.K. Ng^a, R.D. Jenkins^b

^a*School of Mechanical and Aerospace Engineering, Nanyang Technological University, Nanyang Avenue, Singapore, Singapore 639798*

^b*The Dow Chemical Company, UCAR Emulsion Systems, 410 Gregson Drive, Cary, NC 27511, USA*

Received 29 October 2004; received in revised form 21 February 2005; accepted 9 March 2005

Available online 21 April 2005

Abstract

The shear imposed oscillation technique was employed to probe the shear-induced structural changes of various model associative polymers in the shear-thinning and shear-thickening regimes. The shear-thickening behavior is related to the transformation from predominantly intra-molecular to inter-molecular associations. The shear-thinning behavior under moderate shear deformation is caused by the reorganization of the transient network structure. Under high shear deformation, the shear-thinning behavior is caused solely by the shear-induced effect that increases the chain-end exit rate, which reduces the mechanical active chains and lifetime of the hydrophobe in the micellar junctions.

© 2005 Elsevier Ltd. All rights reserved.

Keywords: Polyelectrolyte; Hydrophobic; Relaxation

1. Introduction

The increasing concerns on the environmental impact regarding the use of organic solvents has provided strong impetus for the shift in the development of coating technology, i.e. such as the replacement of solvent with water-borne coating systems. One critical parameter defining the performance of these coatings, particularly paints, is their rheology. At low shear, it requires high viscosity to prevent pigment sedimentation during storage as well as controlling the flow, leveling of the paint and its sag resistance after application. At the moderate shear condition, a moderate viscosity is required to allow loading of brush and roller as well as to ensure the optimum pouring and mixing behavior. Low viscosity is required at high shear condition to achieve film build property to achieve high gloss quality [1].

Due to the limitations of non-associative polymers, such as cellulose ether, associative polymer was introduced in 1973 to confer better overall rheological properties to the

paints, primarily on improving flow and leveling behavior. Hydrophobically modified alkali-soluble (HASE) associative polymer has received increasing attentions in recent years [2–21]. Most of these studies focused on describing the microstructure and the behavior of HASE in the presence of surfactants. There is, however, few studies that focus on the rheological behavior of HASE polymer under various deformation conditions. In order to develop a clearer understanding on the rheological properties of HASE polymer under varying deformation, the superposition oscillation technique described by Tirtaatmadjia et al. [4] can be utilized to provide qualitative understanding on the microstructure of the system. Tirtaatmadjia et al. [5] showed that the relaxation behavior of the HASE polymer shifted to faster relaxation time upon the application of stress. This behavior was believed to be dependent on the state of network disruption and re-organisation of the hydrophobic junctions. The application of this technique to the HEUR system [22], showed that the reduction in the relaxation time is a consequence of lower junction densities and shear-enhanced exit rate of the hydrophobic groups from the micellar junctions of the network.

The main motivation of this paper is to incorporate the superposition oscillation technique with the relaxation spectrum analysis on the HASE to provide an in-depth

* Corresponding author. Fax: +65 6791 1859.

E-mail address: mkctam@ntu.edu.sg (K.C. Tam).

understanding on the structural behavior of the system under various shear deformations.

2. Material and experimental methods

The model associative polymers examined in this study are hydrophobically modified, alkali-soluble (HASE) polymers synthesized by Dow chemicals (formerly Union Carbide), via the emulsion polymerization process of methacrylic acid (MAA), ethyl acrylate (EA) and a macromonomer that had been capped with a hydrophobic group. The chemical structure of the polymer is shown in Fig. 1, where R is C_nH_{2n+1} . The polymer characterizes in this paper are HASE05-20 and HASE40-20. The difference between the two polymers is the length of the ethylene-oxide spacer chain of the macromonomer. The ethylene-oxide spacer chain length of HASE05-20 is 4.2 moles, while the spacer chain length of HASE40-20 is 41.6 moles. The hydrophobes of the polymers are identical, consisting of $C_{20}H_{41}$ alkyl chain.

A brief description of the synthesis methodology of the model polymer has been previously reported [2,5] and will not be presented here. The characteristics and chemical composition of the model polymer are given in Table 1. The molecular weight of the model associative polymer was determined to be $\sim 200,000$ Daltons [23,24], and the monomer sequence distribution of these polymers are believed to be quite similar, since the process used to produce them was held constant.

The samples were prepared from a stock solution of 3 wt% of total solid polymer solids in 10^{-4} M KCl adjusted to the required concentration. The alkaline used to neutralize the polymer to the required pH ~ 9.0 was 2-amino-methylpropanol (AMP). This is to ensure complete neutralization of the polymer where maximum enhancement of the rheological properties was observed [7,11]. The steady shear viscosity of HASE40-20 displays a shear-

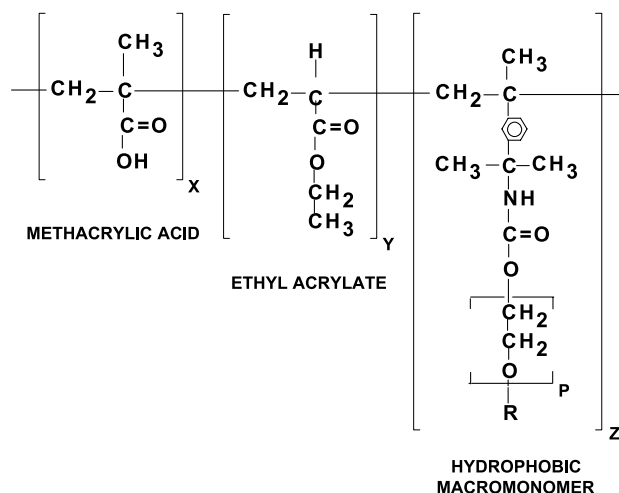


Fig. 1. Chemical Structure of model HASE Polymer.

Table 1
Details on chemical composition of model HASE polymers

Name of HASE	Moles of EO	Hydrophobes name	Hydrophobes formula	Molar ratio of MAA/EA/macromonomer
HASE05-20	4.2	Eicosanyl	$C_{20}H_{41}$	49/50/1
HASE40-20	41.6	Eicosanyl	$C_{20}H_{41}$	49/50/1

thickening regime at moderate shear rates, however, the viscosity of HASE05-20 decreases progressively with shear rates as shown in Fig. 2.

Superposition of oscillation on shear technique was employed using the Controlled Stress Carri-Med CSL500 rheometer for determining the structural behavior at various stages of applied stresses. The geometry used with the CSL500 is a cone and plate system with diameter 40 mm and 2° cone angle. Characterization of the polymeric systems was carried out with a circulating water bath to ensure constant temperature of 25°C throughout the samples during each experiment.

3. Results and discussion

The structural properties of associative polymers, which possess shear-thickening and shear-thinning or combination of both behaviors under shear deformation were investigated. In order to obtain detailed structural information, the superposition of oscillation on shear technique was employed [4,5,8,22]. A shear stress was applied for a fixed time period and once the equilibrium condition was achieved, a superimposed oscillation was applied to probe the viscoelastic behavior of the solution. Using this technique, the viscoelastic response of large network elements and fast response of the dynamic cluster under different applied stresses can be determined by computing the relaxation time spectra.

The dynamic properties of 3 wt% HASE05-20 and HASE40-20 were plotted in Fig. 3(a) and (b), respectively.

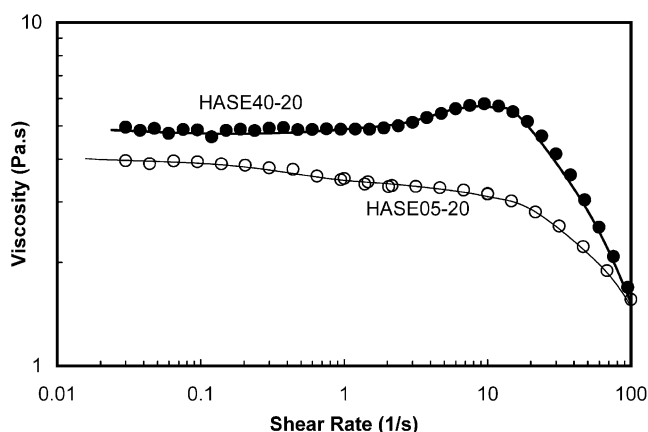


Fig. 2. Shear dependent viscosity of 3.0 wt% HASE05-20 and HASE04-20.

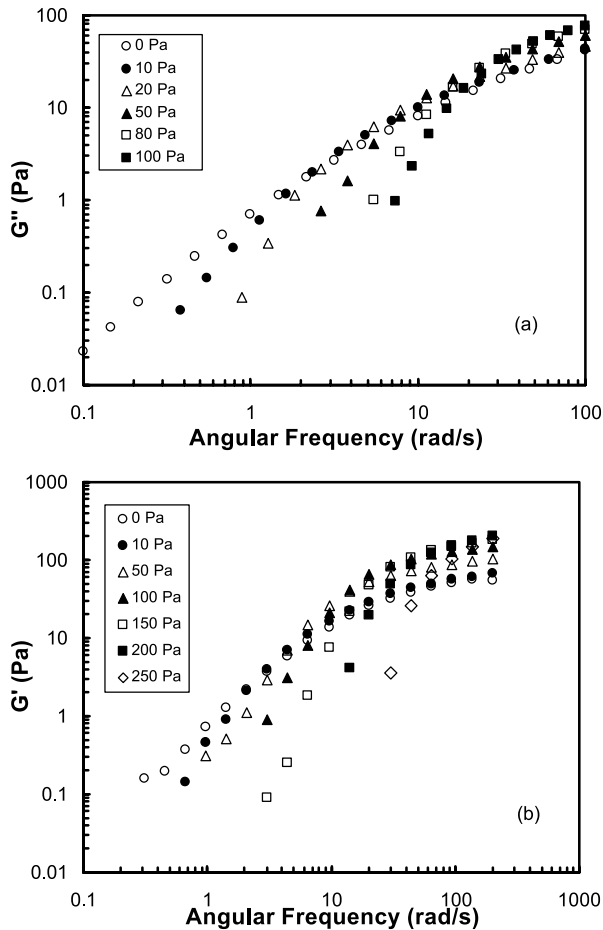


Fig. 3. Linear viscoelastic properties of HASE40-20 at 3.0 wt% at applied stress of (a) 0–100 Pa; (b) 0–250 Pa.

Upon the application of stresses, the terminal region shifts to higher frequencies. The dynamic data were fitted with the multiple modes Maxwell model equation as shown in Figs. 4(a–d) and 5(a–d), where the solid lines represents the best fit for the Maxwell model. The generalised Maxwell model/Maxwell–Wiechert model, modified from the simple Maxwell model by connecting a series of spring and dashpot in parallel is represented as follows;

$$G'(\omega) = \sum_{i=1}^N \frac{G_i \omega_i^2 \lambda_i^2}{1 + \omega_i^2 \lambda_i^2}$$

$$G''(\omega) = \sum_{i=1}^N \frac{G_i \omega_i \lambda_i}{1 + \omega_i^2 \lambda_i^2} \quad (1)$$

where the subscript i is used to denote the number of repeated simple Maxwell elements. Usually, N ranges from 1 to 3, signifying that there are 1–3 different relaxation modes as defined by the fitted relaxation times. Good fits to the data are observed for conditions of zero or low applied stresses. However, at higher stresses, where the viscosity begins to decrease significantly, the Maxwell model is less

able to describe the viscoelastic behavior of the solution. In order to ensure the dynamic data at different shear stresses reflect the true material properties, the oscillatory steady shear viscosity was then compared with the equilibrium shear viscosity as shown in Figs. 6 and 7 for HASE05-20 and 4020, respectively. This gives us the confidence that the dynamic frequency sweep data can be used to describe the structural behavior of the polymer systems using the transformed relaxation time spectra. It is important to note that the storage modulus data plotted in Fig. 3(a) and (b) were obtained from the linear viscoelastic region. Hence, any changes in the rheological properties are not a consequence of non-linear deformations.

In order to establish an understanding on the strength of the network structure, we need to quantify the junction densities and relaxation behavior of the polymer system. Based on Green and Tobolsky theory [25] on rubber elasticity, the G' at high frequency can be used to represent the junction densities in the transient network system. Green and Tobolsky [25] extended the simple theory of rubber elasticity to transient networks where the magnitude of the plateau modulus G_N^0 is related to the number of the effective chains per unit volume ν ;

$$G_N^0 = g\nu RT \quad (2)$$

where g is a correction factor whose magnitude is unity [26], G_N^0 is the plateau modulus, R is the gas constant and T the temperature in Kelvin.

The terminal relaxation time can be determined from the expression;

$$\lambda = \lim_{\omega \rightarrow 0} \left(\frac{G'}{\omega^2 \eta'} \right) \quad (3)$$

where η' is the dynamic viscosity, and the plateau in λ versus ω curve, which corresponds to the terminal region in the G' and G'' plot gives an estimate of the average terminal relaxation time of the material.

The shear-thinning behavior upon the application of shear stress exhibited by most HASE polymer system, except HASE40-20, is believed to be related to the curtailing of the longest relaxation time [5]. In order to have a better picture on the structural behavior of the polymeric systems under shear deformation, the 3 wt% HASE05-20, was subjected to parallel superposition oscillation experiments. At the applied stresses of 5–100 Pa, the storage moduli and the active junction densities of the polymer system increase with the application of the shear stress (Fig. 8(a)). However, the strength of the network structure, based on the activation energy plot, remains constant over this range of applied stresses. The activation energy can be used to quantify the strength of the polymer network, where E_a is the total energy contributed by lifetime of the hydrophobic junction and junction densities in the network [27,28]. The Arrhenius expression of the viscosity can be described by the following equation,

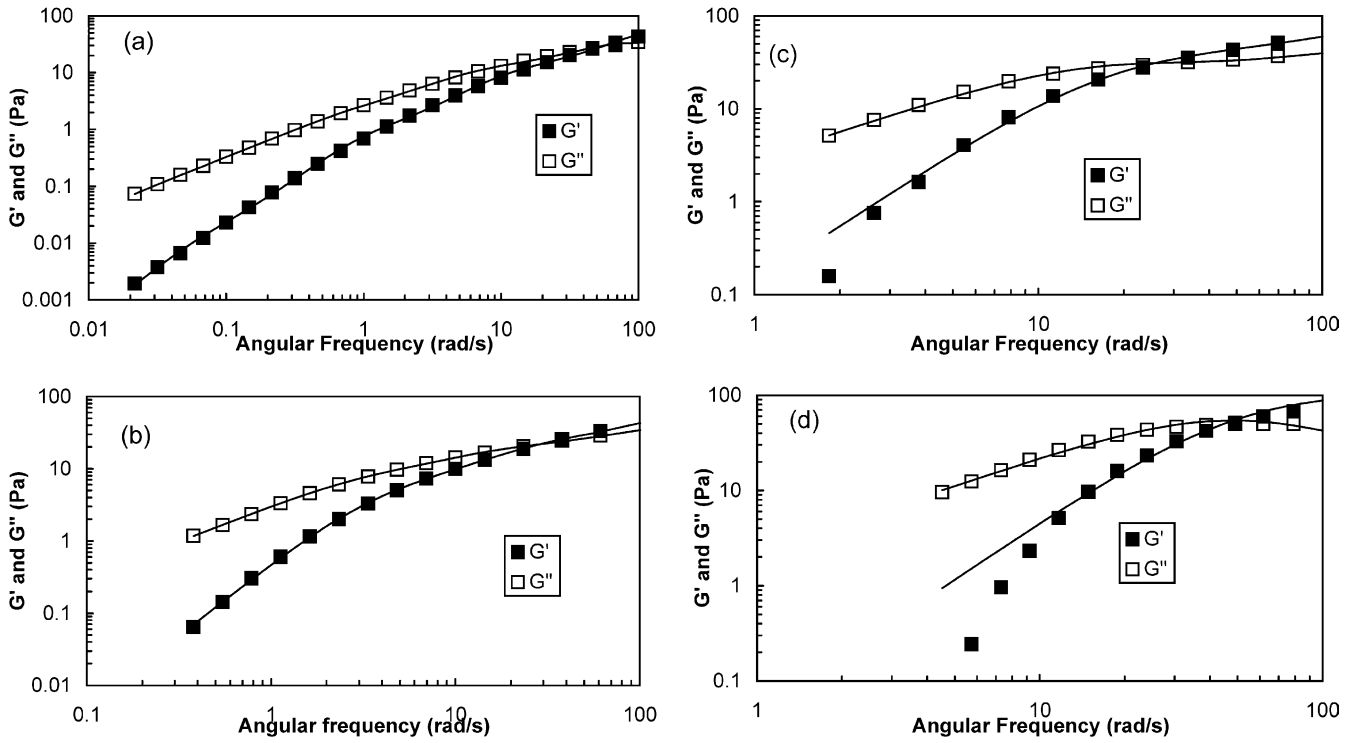


Fig. 4. Fitting of Maxwell model to the dynamic properties of 3.0 wt% HASE05-20 at (a) 0 Pa, (b) 10 Pa, (c) 50 Pa, (d) 100 Pa applied stresses.

$$\eta_0 = \frac{\nu kT}{\omega_0} \exp\left(\frac{E_a}{kT}\right) \quad (4)$$

where ω_0 is the natural frequency of thermal vibration of the

reactive group in an isolated state, k the Boltzmann constant and T the absolute temperature and η_0 is the zero shear viscosity.

The strength of the network is defined as the total

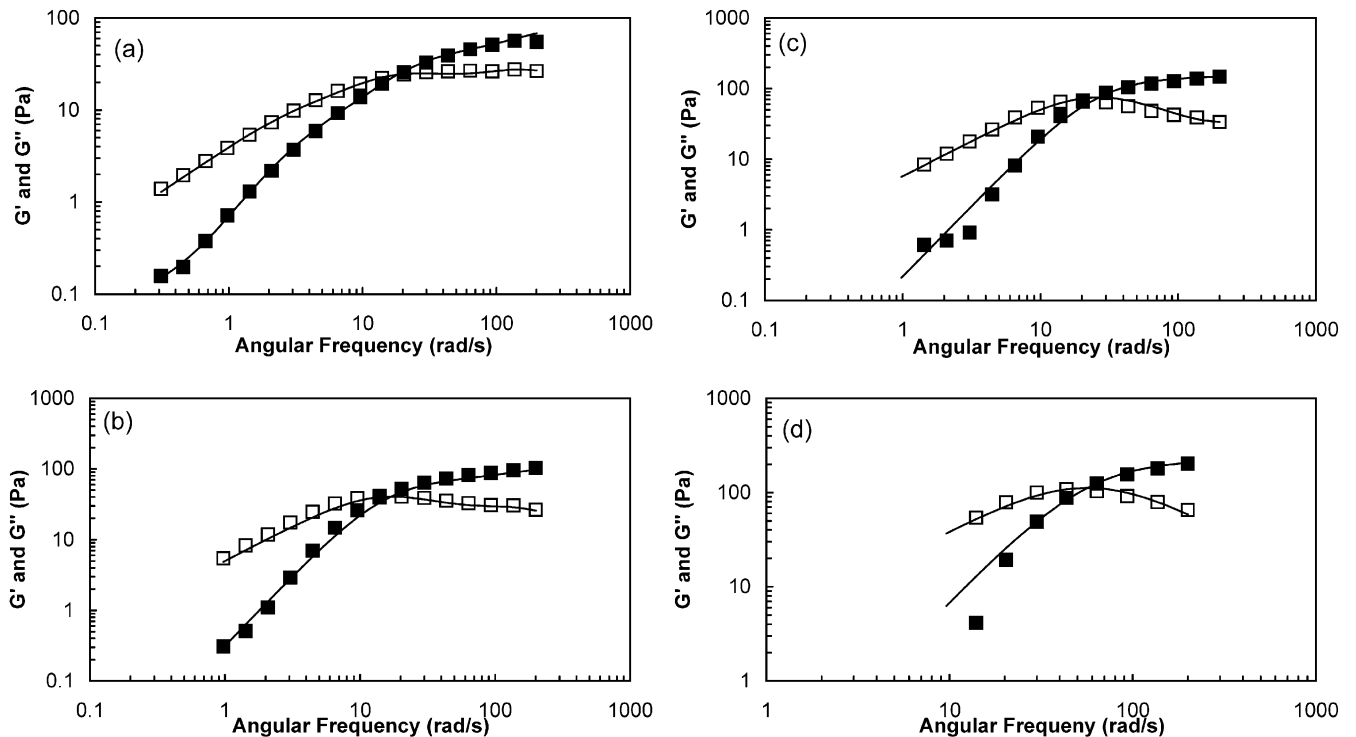


Fig. 5. Fitting of Maxwell model to the dynamic properties of 3.0 wt% HASE40-20 at (a) 0 Pa, (b) 50 Pa, (c) 100 Pa, (d) 200 Pa applied stresses.

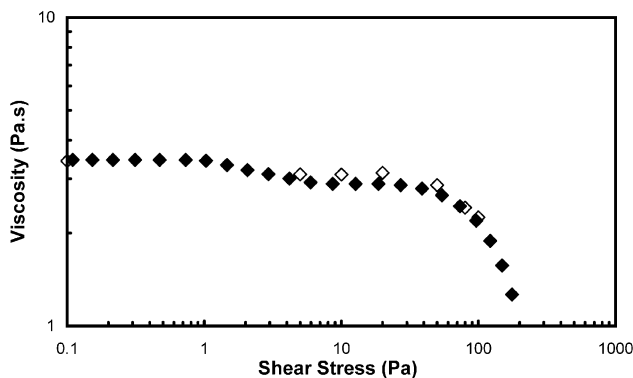


Fig. 6. Comparison of viscosity HASE05-20, 3.0 wt%: equilibrium shear viscosity (closed symbol), oscillatory steady shear viscosity (open symbol).

contribution from the strength of the hydrophobic junctions and the active junction densities in the network [10]. Therefore, the decrease in the network strength caused by the reduction in relaxation time (Fig. 8(b)) is compensated by the increase of junction densities (Fig. 8(a)), leading to a constant activation enthalpy in this range of applied stresses. Above the shear stress of 100 Pa, where the viscosity decreases sharply, the activation energy of the polymer system exhibits a large drop. The reduction in the strength of the network is mainly due to the lost of network connectivity and the reduction in lifetime of the junctions. Hence, it is expected that the storage modulus and average terminal relaxation time will decrease accordingly. However, due to the sensitivity and limitation of the equipment, the dynamic data above 100 Pa could not be measured.

The shear-thickening behavior in HASE40-20 warrants further discussion here. This shear thickening property has been attributed to the transformation of intra- to inter-molecular association. The dynamic properties of HASE40-20 at different applied stresses were measured to clarify the mechanism derived from previous studies. [13,22]. Fig. 9(a) reveals that when the applied stress was increased from 5 to 175 Pa, the junction densities in the network increase continuously. However, the strength of the network as indicated by the activation energy remains constant until an applied stress of 60 Pa. It then increases significantly over

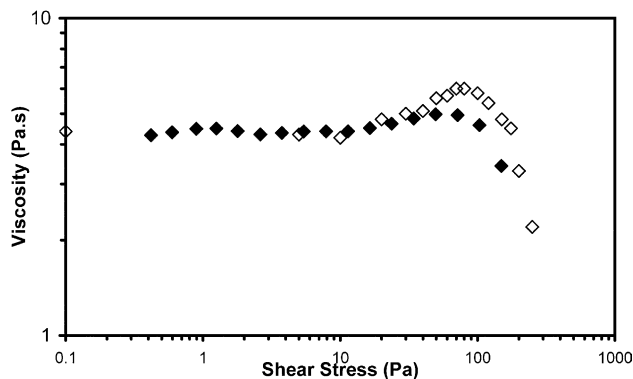


Fig. 7. Comparison of viscosity HASE40-20, 3.0 wt% equilibrium shear viscosity (closed symbol), oscillatory steady shear viscosity (open symbol).

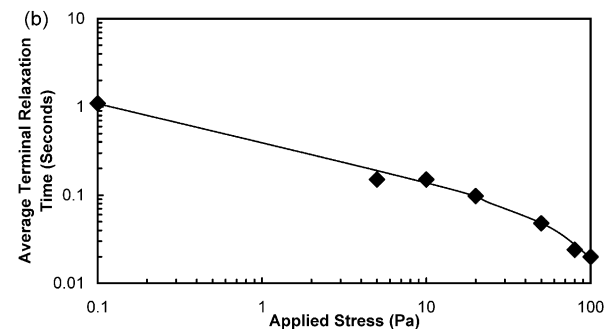
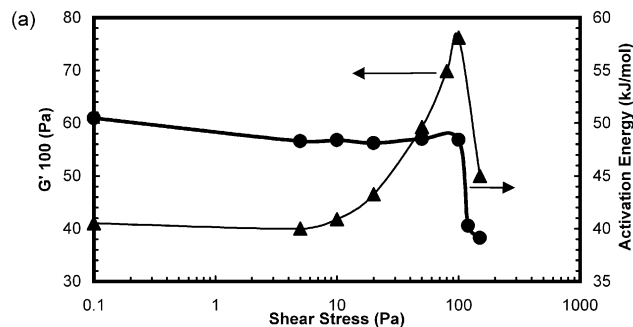


Fig. 8. (a) Storage modulus at 100 rad/s and activation energy as a function of shear stress for 3.0 wt% HASE05-20; (b) average terminal relaxation time as a function of applied stress for 3.0 wt% HASE05-20.

the shear-thickening region. On the other hand, the overall relaxation time of the polymer system in Fig. 9(b) displays the same behavior as HASE05-20, where it decreases with the applied stresses. What then is the cause for the increase in the activation energy and shear-thickening behavior observed in the 3 wt% HASE40-20 which is not present in the HASE05-20 system? By comparing the normalized storage modulus and activation energy determined from viscosity measurements in Fig. 10(a) and (c), it is evident that the rate of increase in the junction densities and enthalpy for HASE40-20 is higher. In addition, the normalized relaxation time plot (Fig. 10(b)) demonstrates that HASE40-20 possesses a higher resistant to shear deformation as depicted by the slower reduction rate of decrease in the relaxation time compared to HASE05-20. The above observations clearly show that the increase in the strength of the network in the shear-thickening region is caused by the formation of greater number of active junctions in the network. One would then ask as to 'where do this additional junction densities come from?' One probable source of the additional junction densities is the conversion of intra- to inter-molecular associations. As HASE40-20 possesses the longest ethylene-oxide linkage (41.6 moles) compared to the rest of the model polymeric systems, the probability of intra-molecular interaction is the highest since, the hydrophobes can extend to a greater distant and associate with another hydrophobes on the same polymer backbone. The formation of larger number of

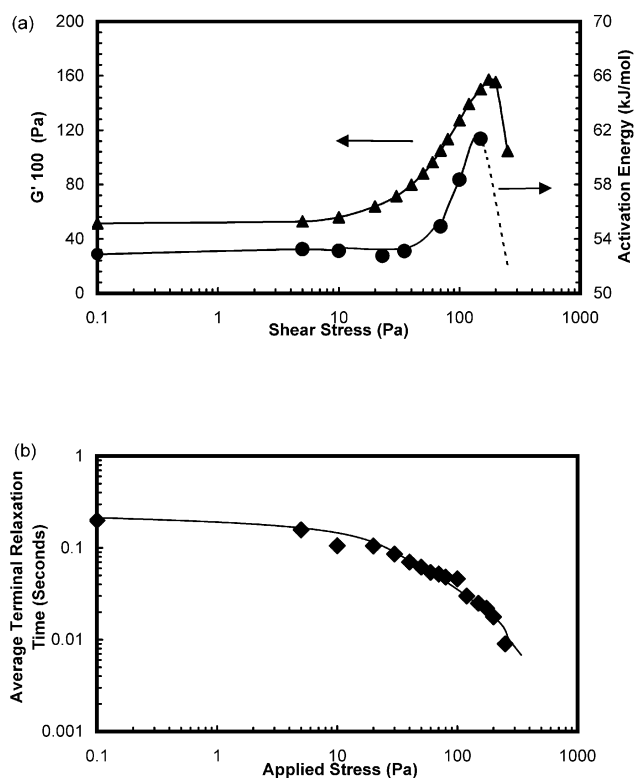


Fig. 9. (a) Storage modulus at 100 rad/s and activation energy as a function of shear stress for 3.0 wt% HASE40-20; (b) Average terminal relaxation time as a function of applied stress for 3.0 wt% HASE40-20.

intra-molecular association in the network causes the polymer to coil into a more compact conformation. Upon application of stress, the polymer backbones unfold, and disrupt the intra-molecular junctions, making available greater number of 'free' or unassociated hydrophobes which can then form inter-molecular junctions with other hydrophobes in the system. The net result is the apparent increase in the network junction density, which contributes to the strength of the network structure. Above 175 Pa of applied stress, the drastic reduction in the rheological properties observed in Figs. 7 and 9(a) is mainly due to the lost of network connectivity and the reduction in lifetime of the structure.

In order to have a better understanding on the relaxation behavior of the polymeric system, the determination of relaxation time, spectrum is necessary. The viscoelastic response of the polymer can be better described by examining the distribution of the relaxation times [10,22,29]. Information on the relaxation spectrum $H(\lambda)$ can be derived by transforming the data obtained in the frequency domain according to the expressions below:

$$G'(\omega) = \int_{-\infty}^{\infty} H(\lambda) \left[\frac{\omega^2 \lambda^2}{1 + \omega^2 \lambda^2} \right] d(\ln \lambda)$$

$$G''(\omega) = \int_{-\infty}^{\infty} H(\lambda) \left[\frac{\omega \lambda}{1 + \omega^2 \lambda^2} \right] d(\ln \lambda) \quad (5)$$

The relaxation time spectrum was mathematical

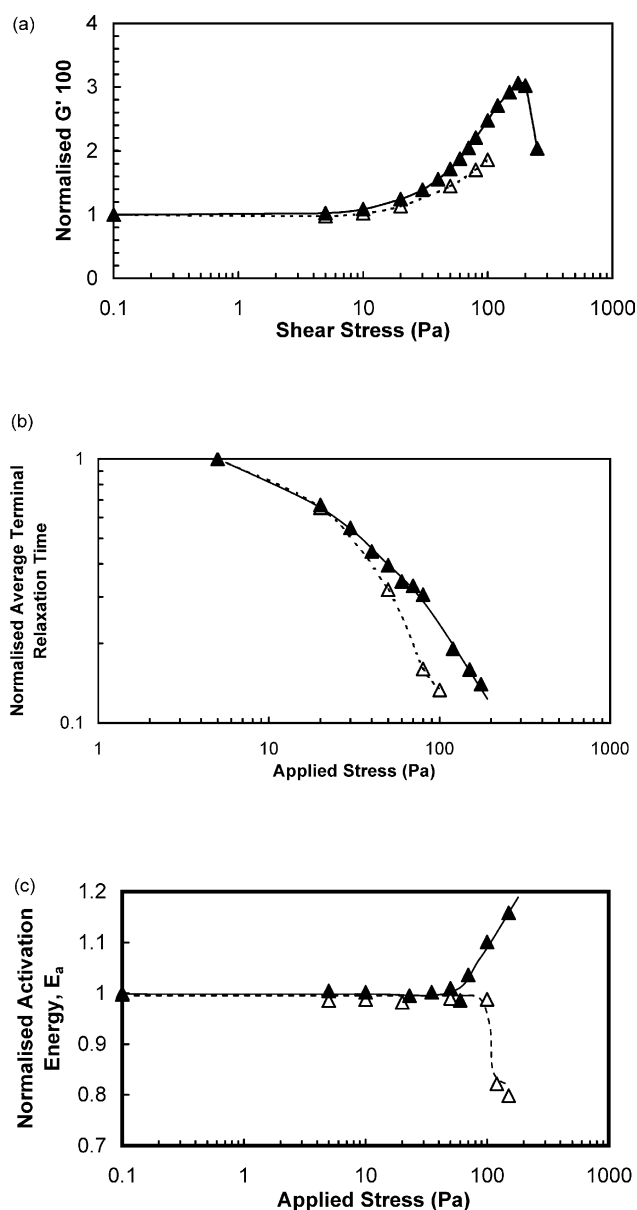


Fig. 10. (a) Normalised storage modulus at 100 rad/s, (b) normalised average terminal relaxation time, (c) normalised activation energy: 3.0 wt% HASE05-20 (open symbol), 3.0 wt% HASE40-20 (closed symbol).

computed using commercial software provided by Rheometric Scientific Inc. (Orchestrator software). The spectra obtained from the storage and loss modulus at different temperatures were plotted as $H(\lambda)\lambda$ versus λ .

In order to have more detailed understanding on the structural property of the HASE polymeric systems under shear deformation, the relaxation behaviors were investigated by the examining the relaxation spectra as shown in Figs. 11 and 12. Upon the application of shear deformation, the width of the relaxation time spectrum decreases and the relaxation peaks shift to shorter times. However, due to the limitation of the equipment, the relaxation time lower than 0.01 s cannot be measured, hence, the spectra at relaxation

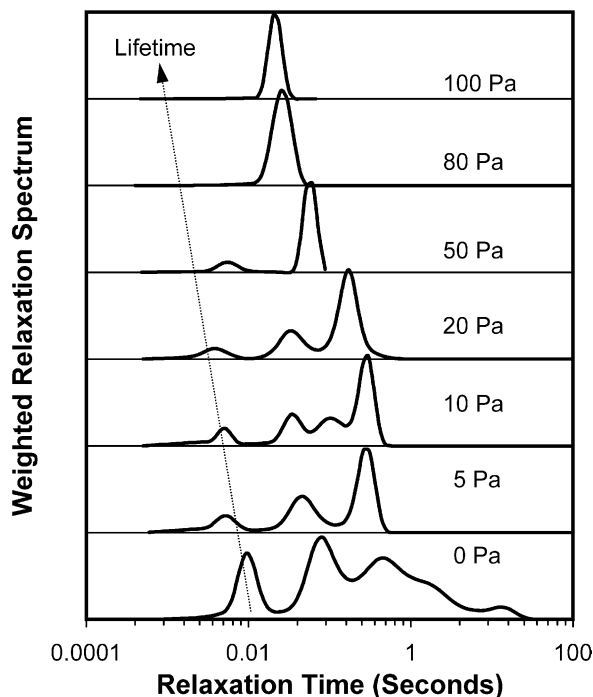


Fig. 11. Weighted relaxation spectrum for 3 wt% HASE05-20 at varying applied stresses.

time lower than 0.01 s and also at higher applied stress cannot be determined. It is evident that at lower shear deformation, the lifetime of the polymer system continues to decrease with increasing deformation as indicated by the dotted line in Fig. 11. The reduction in the lifetime, as represented by the fast peak at short times, indicates that the long relaxation time connected to the junctions with high aggregation number is disrupted. This disruption leads to the re-organization of the network structure, which has the effect of narrowing the distribution of the aggregation number in the associating junctions. The net result is the overall reduction in both the lifetime and structural relaxation time of the polymer network. In addition, free hydroprobes from the disrupted junctions re-associate to form junctions with lower aggregation number, which raises the number of mechanically active junctions in the polymer network (Figs. 8(a) and 9(a)). Deformation of the HASE polymer at higher stresses results in the overall reduction of junction densities, junction strength, lifetime and relaxation time of the system. This behavior corresponds to the transient network theory proposed by Tanaka and Edwards [28,30]. They stated that the exit rate of the hydrophobe depends on the applied stress, which is enhanced by the application of stress. This indicates that the applied stress is sufficiently high to decrease the lifetime of the micellar junction. Hence, the drastic decline in the viscosity profile observed for both polymeric systems, is caused by the increase in the chain-end exit rate due to applied stress.

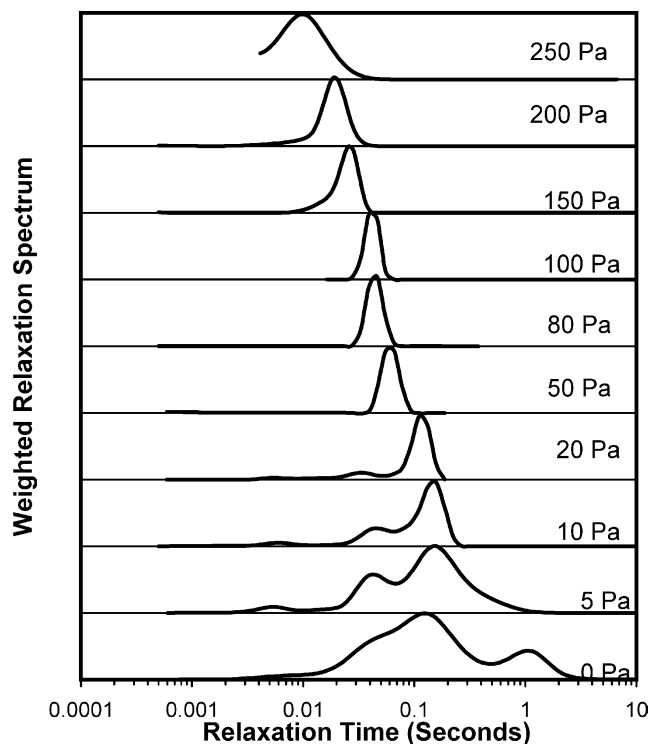


Fig. 12. Weighted relaxation spectrum for 3 wt% HASE40-20, at varying applied stresses.

4. Conclusions

The superposition of oscillation on steady shear experiment provides insights into the state of the network structure under shear deformation. With increasing applied stresses, the junction densities increase but the overall relaxation time of the system decreases. The rate of increase in the junction densities and the reduction in the relaxation time defines the onset in the shear-thinning or thickening behavior. The shear-thickening behavior corresponds to the transformation of the predominantly intra-molecular associations to inter-molecular associations. The shear-thinning behavior under moderate shear deformation is caused by the re-organization of the transient network structure. At high shear stresses, it is caused by the enhanced shear-induced chain-end exit of the hydrophobes from the junction, which reduces the mechanical active chains and lifetime of the hydrophobe in a micellar junction.

Acknowledgements

We would also like to acknowledge the financial support provided by the the Ministry of Education and the Agency for Science, Technology and Research, Singapore.

References

- [1] Sperry PR, Thibeault JC, Kotansek EC. Proceedings of the 11th

- International Conference on organic coating and technology, Athens, Greece. Advanced organic coating science technology series 1987. p. 1.
- [2] Jenkins RD, Delong LM, Basset DR. In: Glass JE, editor. Hydrophilic polymers, influence of alkali-soluble associative emulsion polymer architecture on rheology. Advances in chemistry 248. Washington, DC: ACS; 1996. p. 425.
- [3] Guo L, Tam KC, Jenkins RD. Macromol Chem Phys 1998;199:1175.
- [4] Tirtaatmadja V, Tam KC, Jenkins RD. Macromolecules 1997;30(5): 1426.
- [5] Tirtaatmadja V, Tam KC, Jenkins RD. Macromolecules 1997;30(5): 3271.
- [6] Tirtaatmadja V, Tam KC, Jenkins RD. AIChE J 1998;44(12):2756.
- [7] Kumacheva E, Rharbi Y, Winnik MA, Guo L, Tam KC, Jenkins RD. Langmuir 1997;13:182.
- [8] English RJ, Gulati HS, Jenkins RD. J Rheol 1997;41(2):427.
- [9] Ng WK, Tam KC, Jenkins Richard D. Eur Polym J 1999;35(7):1245.
- [10] Ng WK, Tam KC, Jenkins RD. Polymer 2001;42:249.
- [11] Tam KC, Farmer ML, Jenkins RD, Bassett DR. J Polym Sci Part B, Polym Phys 1998;36:2276.
- [12] Seng WP, Tam KC, Jenkins RD. Colloids Surf, A 1999;154(3):363.
- [13] Tam KC, Guo L, Jenkins RD, Bassett DR. Polymer 1999;40(23):6369.
- [14] Horiuchi K, Rharbi Y, Spiro JG, Yekta A, Winnik MA. Langmuir 1999;15:1644.
- [15] Tam KC, Ng WK, Jenkins RD. J Appl Polym Sci 2004;94:604.
- [16] Dai S, Tam KC, Jenkins RD. Macromol Chem Phys 2002;203:2312.
- [17] Wang C, Tam KC, Jenkins RD. J Phys Chem B 2002;106:1195.
- [18] Dai S, Tam KC, Jenkins RD. Macromol Chem Phys 2001;202:335.
- [19] Abdala AA, Wu W, Olesen KR, Jenkins RD, Khan SA. J Rheol 2004; 48:979.
- [20] Abdala AA, Olesen KR, Khan SA. J Rheol 2003;47:497.
- [21] English RJ, Raghavan SR, Jenkins RD, Khan SA. J Rheol 1999;43: 1175.
- [22] Tam KC, Jenkins RD, Winnik MA, Bassett DR. Macromolecules 1998;31:4149.
- [23] Islam MF, Jenkins RD, Bassett DR, Lau W, Ou-Yang HD. Macromolecules 2000;33:2480.
- [24] Dai S, Tam KC, Jenkins RD. Macromolecules 2000;33:404.
- [25] Green MS, Tobolsky AV. J Chem Phys 1946;15:80.
- [26] Jenkins RD, PhD Thesis. The fundamental thickening mechanism of associative polymers in latex system: a rheological study, Lehigh University, Bethlehem, PA; 1990.
- [27] Annable T, Buscall R, Ettelaie R, Whittlestone D. J Rheol 1993;37: 695.
- [28] Tanaka F, Edwards SF. J Non-Newton Fluids Mech 1992;43:247.
- [29] Ferry JD. Viscoelastic properties of polymers. 3rd ed. New York: Wiley; 1980.
- [30] Tanaka F, Edwards SF. J Non-Newton Fluid 1992;43:273.